

Pixel-matched holographic data storage with megabit pages

R. M. Shelby, J. A. Hoffnagle, G. W. Burr, C. M. Jefferson, M.-P. Bernal, H. Coufal, R. K. Grygier, H. Günther, R. M. Macfarlane, and G. T. Sincerbox

IBM Almaden Research Center, 650 Harry Road, San Jose, California 95120-6099

Received June 17, 1997

Digital data-page holograms consisting of 1024×1024 arrays of binary pixels have been stored and subsequently retrieved with an optical exposure consistent with a data rate 1 Gbit/s. Each input pixel was precisely registered with a single detector pixel, and a raw bit-error rate as low as 2.4×10^{-6} was demonstrated with global-threshold detection. To our knowledge, this is the first demonstration of the often-cited goal of holographic data storage of megabit data pages and a gigabit-per-second data rate. © 1997 Optical Society of America

Digital holographic data storage, first conceived nearly 30 years ago,^{1,2} has received a great deal of attention recently.³⁻⁸ This is due largely to the emergence of liquid-crystal spatial light modulator and CCD detector-array technologies, which provide suitable input and output and thus allow one to seriously consider holography for data storage. One important feature of holographic storage is its high degree of parallelism, which arises from the storage and retrieval of holograms consisting of two-dimensional arrays, or pages, of binary pixels.

It is projected that holographic storage can take advantage of this parallelism to achieve data rates in the gigabit-per-second (Gbit/s) range. Both spatial light modulators and CCD's are available with 1024×1024 arrays of pixels and 1-kHz frame rates, and these yield an attractive data rate of 1 Gbit/s. If 1000 such pages could be stored in a volume with a cross section of roughly 5 mm, an areal density of 4 Gbits/cm² would be achieved, which is very competitive with current magnetic storage technology. The raw bit-error rate (BER) must be better than $\sim 10^{-5}$, a level correctable to 10^{-12} with an acceptable overhead for error-correcting code. Although they are often-cited goals,^{6,8-10} the storage and retrieval of megabit (Mbit) holograms at such an error rate have never been accomplished to our knowledge, nor has a demonstration of Gbit/s readout. This is because the precise imaging of each input data pixel over the entire 1024×1024 array through the storage medium and onto the corresponding detector pixel requires resolution and distortion performance that is usually unobtainable with inexpensive optics. Furthermore, Mbit-per-page holographic storage demands very high optical quality of the storage medium and excellent fidelity of the holographic recording and reconstruction process.

With the holographic storage tester described in Ref. 6, a small number of Mbit data pages were stored and retrieved in iron-doped lithium niobate (LiNbO₃) crystals. The high optical performance of this tester permits precise one-to-one pixel matching from input data mask to detector array, and decoding of the reconstructed data-page image with a simple global threshold yielded BER's as low as 2.4×10^{-6} . The holograms had a diffraction efficiency of $\eta = 3 \times 10^{-5}$ to 4×10^{-4} and could be read out with a 1-ms exposure

of the readout beam, yielding an effective optical data rate of 1 Gbit/s.

The input data pattern was provided by a chrome-on-glass transmission mask consisting of a two-dimensional array of pixel locations spaced 9 μ m apart. At approximately half of the randomly selected locations a 4.5- μ m square opening was etched into the chrome to represent a binary 1 pixel. The other half of the pixels represented 0. The data pattern was imaged through the LiNbO₃ crystal onto a CCD detector array with two custom lenses of approximately 89-mm effective focal length in the usual 4*f* Fourier holography configuration. The crystal was located approximately 2 cm behind the Fourier plane of the lens system. The optics produced a pixel-matched, unity-magnification image of the data mask on the Kodak CCD that consisted of a 1536×1024 array of 9- μ m detector pixels.

Two iron-doped LiNbO₃ crystals were used, each 15 mm \times 15 mm \times 8 mm in size. The object beam entered through the 15 mm \times 15 mm face, and the reference beam at 90° through one of the 8 mm \times 15 mm faces, after expansion with cylindrical optics to nearly fill the crystal volume. Both beams were *o* polarized. Both crystals were doped with 0.02% iron and had an absorptivity of 0.8 cm⁻¹ at 514 nm. We erased the crystals before experimental runs by heating them to 200 °C for 1 h. One crystal was *xyz* cut with the *c* axis parallel to a 15-mm edge and in the plane of incidence of the object and the reference beams. The second crystal had its *c* axis at 45° to the object and the reference beams and in the plane of incidence.

The *xyz*-cut crystal had nearly an order-of-magnitude lower sensitivity than the 45°-cut crystal in this 90° geometry. In the *xyz*-cut sample the best holograms were typically written for 2 min with reference-beam power of 30 mW/cm² and average object-beam power of 0.3 mW/cm², yielding a diffraction efficiency of $\eta \approx 10^{-5}$. For the 45° crystal, 70–100-s exposures with powers of 39 mW/cm² (reference) and 0.24 mW/cm² (object) yielded $\eta \approx 4 \times 10^{-4}$. Multiple exposures were angle multiplexed at 0.1° spacing, more than an order of magnitude greater than the width of the Bragg peak, and thus interpage cross talk was negligible. For readout, the camera shutter was opened, and the reference beam was then pulsed

with an acousto-optic modulator for ≥ 1 ms. The CCD signal was digitized by a Princeton Instruments ST138 camera with 14-bit precision.

Since the locations of all 1 and 0 pixels are known *a priori*, an intensity distribution function (or histogram) can be built for the 1's and for the 0's, and the extent of their overlap determined. A global threshold was selected that minimized the sum of the number of 1 pixels with intensities below the threshold and the number of 0 pixels with intensities above the threshold. When the distributions of 1's and 0's were well separated and there were no errors, we estimated the error rate by fitting the tails of the distributions with Gaussians and calculating the probability of overlap.⁶

When imaging the megapixel data mask directly onto the CCD array through high-optical-quality fused silica instead of the LiNbO₃ crystal, the tester is capable of an error rate of better than 10^{-8} , limited by residual distortion and variations in the input illumination intensity. When the LiNbO₃ crystal is inserted into the object beam, the error rate increases to 3.4×10^{-6} , partly owing to the spatial filtering of the object beam by the 15-mm crystal aperture but also to the optical imperfections of even the best available LiNbO₃. The best error rate achieved for a Mbit hologram was 2.4×10^{-6} , essentially identical to that for the image.

Figure 1 shows a comparison of the histograms of the best image and the hologram. This hologram was recorded in the 45° crystal with $\eta = 4 \times 10^{-4}$. The hologram was read by a 1-ms pulse of the reference beam with 70-mW total power, showing the feasibility of a 1-Gbit/s optical data rate. The weakest Mbit hologram that was readable could be read in 1 ms with a BER of $\leq 10^{-5}$, had $\eta = 3 \times 10^{-5}$, and resulted in a signal at the CCD camera of $\approx 15,000$ photons per 1 pixel. In direct-imaging experiments of Mbit data pages, the onset of errors owing to the detector noise floor is observed for signals below ~ 5000 photons per 1 pixel.

The first few holograms could be recorded with high fidelity. However, as subsequent holograms were recorded in the same volume with identical exposures, the error rate increased rapidly, as shown in Fig. 2. For the *xyz*-cut crystal, only a few good holograms could be recorded, whereas for the 45° crystal, two 50-hologram runs were executed. Measurement of erasure owing to subsequent exposures permitted a M/# (Ref. 7) of 0.15 to be estimated. $\eta \approx 10^{-5}$ is needed for Gbit/s readout with reasonable laser power, which implies that ~ 50 holograms could be multiplexed, for a storage density of 35 Mbits/cm².

Most of the errors in the high-error-rate holograms are due to a high-intensity tail on the 0 intensity distribution that grows with exposure and is associated with the onset of distortions or loss of contrast, usually along the edges of the data page, although there were some differences between the two crystals. We have not yet identified the source of the distortion that leads to these errors, but we believe that so-called photovoltaic damage,⁷ which is known to occur in LiNbO₃,¹¹ is a likely candidate. Because of the strong photovoltaic charge transport in this material, the photorefractive response to low spatial frequencies is enhanced relative

to the higher spatial frequencies of the hologram itself. The resulting slowly varying refractive-index variations produce distortions. With the Fourier plane inside the crystal, the very high-intensity regions of the object beam cause severe distortions, even for a single exposure. For the data shown here, the crystal was approximately 2 cm behind the Fourier plane, and we attribute the distortion to the remaining object-beam intensity pattern and to the intensity profile created by reference-beam absorption. In the *xyz*-cut crystal the low-frequency object-beam intensity gradients are oriented along the *c* axis, and the higher sensitivity to distortion for this orientation is likely related to the anisotropy of photorefractive response that we measured between the two orientations.

All these error rates were determined with a single global threshold. Of the errors that arose with increasing exposure, the high 0's and low 1's tended to be in different parts of the page, suggesting that a more locally determined threshold would yield better results. Accordingly, each 1024×1024 data page was divided into nine blocks, as shown in the inset of Fig. 3. When a separate optimum threshold was used for each block, the highest-fidelity holograms could be decoded without error, with a BER of 2×10^{-8} . The error rates of most of the holograms improved by more than an order of magnitude.

In a storage application a modulation coding-decoding scheme would be used, both to avoid the

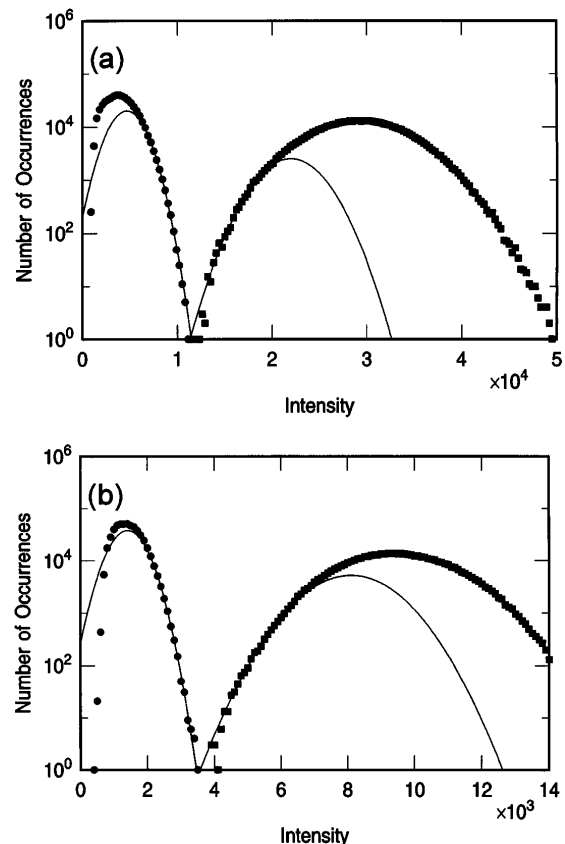


Fig. 1. Histograms of (a) the megabit image and (b) the hologram. Fitting of the tails of the distributions of 0's (circles) and 1's (squares) to Gaussian yields the solid curves and an estimate of the BER of 3.4×10^{-6} for the image and 2.4×10^{-6} for the hologram.

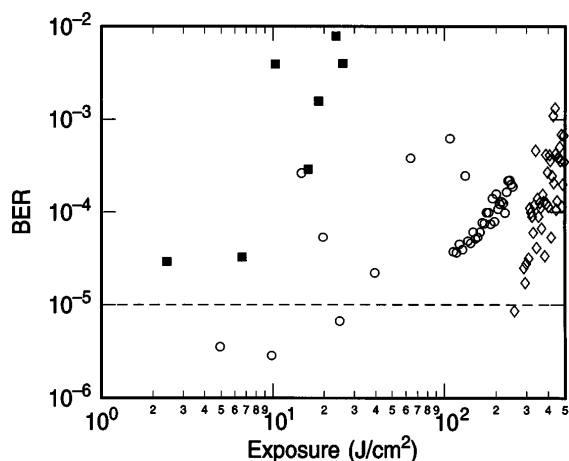


Fig. 2. Increase in the BER with repeated exposure for both xyz and 45° crystals. The dotted line shows the desired raw error rate (10^{-5}). Errors increase more rapidly for the xyz -cut crystal orientation (squares). For the 45° crystal, the circles and diamonds show two 50-exposure runs with a reoptimization of the imaging of the tester in between.

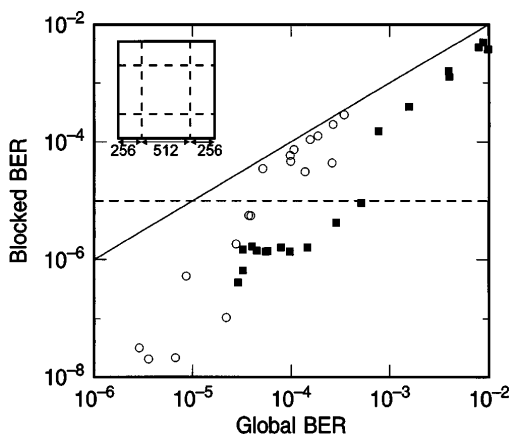


Fig. 3. Improvement in the BER is shown when blocked thresholding is used, with blocks as shown in the inset, compared with the BER with global thresholding. Squares, xyz -cut crystal; circles, 45° crystal.

need to determine a threshold and to reduce errors. In other experiments,⁸ we had good success at lower page density when we used balanced block modulation codes. For example, a block of 8 pixels, half bright and half dark, can code 6 bits of binary data. Decoding depends on only the intensity values within a single block, simplifying decoding. The use of such a code would cost 25% of the data capacity.

To establish a correspondence between a BER determined with the global threshold for a megapixel data page and the expected number of errors for a modulation-coded page, we performed a software remapping of the data pixels within the page of output data. This created a set of valid code words composed of pixels that were located near one another in the actual data mask. Thus, large-scale nonuniformities should be compensated for, as in an actual coded data page. However, if local correlations are somehow important in inducing errors, the simulated block coding might give an invalid estimate of error rate. The random binary data of the megapixel page were grouped

in blocks with two different remappings, corresponding to valid code words in the 6:8 code or a more-powerful 8-bit-12-pixel code.⁸ The modulation-coded pages could generally be decoded with the 6:8 code with no errors for input pages with as many as ~ 20 errors with the global threshold, or as many as ~ 100 errors for the 8:12 code. When a standard error-correcting code was also applied, all errors were corrected up to an input raw (global-threshold) BER of 4×10^{-3} . The combined overhead of these coding schemes resulted in 713,664 (634,368) user bits per megapixel page for the 6:8 (8:12) code.

In summary, digital data holograms containing 10^6 data bits have been stored and recalled in a lithium niobate crystal. The estimated BER when threshold decoding in nine subblocks was used was as low as 2×10^{-8} , whereas simulation of a realistic data-coding scheme gave error-free decoding up to a global-threshold BER of 2×10^{-3} . Holograms of diffraction efficiency greater than 3×10^{-5} were read out with optical integration times of 1 ms.

Recording a sequence of angle-multiplexed megapixel holograms produced a rapid increase in the error rate. We suggest that photovoltaic optical damage in LiNbO_3 is responsible, but the details of this process remain to be investigated.

The estimated M/# for the 45° -cut crystal was 0.15, projecting an areal density of only 35 Mbits/cm² when the need for Gbit/s data rates with reasonable laser power is considered. It should be possible to improve this performance, in particular with more-efficient use of laser power, which would permit higher object-beam intensities, and with higher- f -number optics, which would reduce the volume of material for a single hologram stack. However, the multiplexing of large numbers of holograms in a common volume will be difficult unless the rapid increase of errors shown in Fig. 2 is understood and controlled.

References

1. P. J. van Heerden, *Appl. Opt.* **2**, 393 (1963).
2. F. S. Chen, J. T. L. Macchia, and D. B. Frazer, *Appl. Phys. Lett.* **13**, 223 (1968).
3. G. Sincerbox, in *Current Trends in Optics*, C. Dainty, ed. (Academic, New York, 1994), pp. 195-207.
4. G. Burr, F. Mok, and D. Psaltis, *Opt. Commun.* **117**, 49 (1995).
5. J. Heanue, M. Bashaw, and L. Hesselink, *Science* **265**, 749 (1994).
6. M.-P. Bernal, H. Coufal, R. K. Grygier, J. A. Hoffnagle, C. M. Jefferson, R. M. Macfarlane, R. M. Shelby, G. T. Sincerbox, P. Wimmer, and G. Wittmann, *Appl. Opt.* **35**, 2360 (1996).
7. F. H. Mok, G. W. Burr, and D. Psaltis, *Opt. Lett.* **21**, 896 (1996).
8. G. W. Burr, J. Ashley, H. Coufal, R. K. Grygier, J. A. Hoffnagle, C. M. Jefferson, and B. Marcus, *Opt. Lett.* **22**, 639 (1997).
9. H.-Y. S. Li and D. Psaltis, *J. Opt. Soc. Am. A* **12**, 1902 (1995).
10. D. Psaltis, M. Levene, A. Pu, and G. Barbastathis, *Opt. Lett.* **20**, 782 (1995).
11. A. Glass, D. von der Linde, and T. Negran, *Appl. Phys. Lett.* **25**, 233 (1974).